White Sands Dune Field, New Mexico: Age, dune dynamics and recent accumulations

Gary Kocurek [a,*], Mary Carr [a,1], Ryan Ewing [a], Karen G. Havholm [a,2], Y.C. Nagar [b], A.K. Singhvi [b]

[a] *Department of Geological Sciences, Jackson School of Geosciences, 1 University Station C1100, Austin, Texas 78712, USA*
[b] *Planetary and Geosciences Division, Physical Research Laboratory, Ahmedabad 380 009, India*

Abstract

The White Sands Dune Field, situated within the Tularosa Basin in southern New Mexico, is thought to have been largely derived by a stepwise, progressive deflation of Pleistocene Lake Otero strata with the onset of regional aridity. Optically stimulated luminescence (OSL) dating of samples from a core that penetrated the gypsum accumulation of the dune field confirm a time of origin at ∼7000 yr. Dune sediment is characterized as lagged influx from previously stored Lake Otero sediment and contemporaneous influx derived from subsequent playas. Sediment became available for aeolian transport and dune-field construction because of a falling water table driven by the regional aridity. The current dune field is primarily a wet aeolian system in which the behavior of the accumulation surface over time is a function of the water table, although surface cementation by gypsum also imparts aspects of a stabilizing system. Dune crests are oriented borderline transverse to the annual transport resultant, and a monitored dune and its cross-strata show that transverse winds from the SW during the late winter and spring account for most of the crest-normal migration, but a significant along-crest component of migration of dune sinuosity occurs with fall and winter winds from the NW and N that strike the crests obliquely. Trenches across three interdune areas show dune sets and interdune strata climbing at about 0.1°. Depth of interdune scour increases with interdune streamwise length, which acts to enhance the probability of dune cross-strata deflation during arid years, but also increases the probability of interdune accumulation because the water table shows a net rise over time. Within the trenches, dune sets show a bundling of foresets between reactivation surfaces, interpreted as annual cycles that reveal lee-face reworking by the oblique NW and N winds and slipface progradation fostered by transverse winds from the SW. A progression from grainflow-dominated to wind-ripple-dominated cross-strata within a single set revealed in the longest trench is consistent with along-crest migration of dune sinuosity. Interdune laminations show light/dark couplets interpreted as annual varves reflecting dry/wet portions of the year. The number of laminations preserved in vertical sections across an interdune area shows that the record is incomplete, and endorses the interpretation of periods of interdune deflation. A calculation of the current accumulation rate as based upon the climbing strata within the trenches is significantly greater than the long-term accumulation rate determined by OSL dates taken from the core. In addition to compaction and possible

---

* Corresponding author. Tel.: +1 512 471 5855.
E-mail addresses: garyk@mail.utexas.edu (G. Kocurek), mcarr@mines.edu (M. Carr), rce@mail.utexas.edu (R. Ewing), HAVHOLKG@uwec.edu (K.G. Havholm), ycnagar@prl.res.in (Y.C. Nagar), singhvi@prl.res.in (A.K. Singhvi).
[1] Present address: Department of Geology and Geological Engineering, Colorado School of Mines, Golden, Colorado 80401, USA.
[2] Present address: Department of Geology, University of Wisconsin-Eau Claire, Eau Claire, Wisconsin 54702, USA.

dissolution of gypsum as partial explanations, the long-term accumulation rate may reflect significant variation in the accumulation rate over time, short-term deflation of accumulations on a regular basis, and/or the presence of unconformities within the gypsum body.

1. Introduction

The White Sands Dune Field, situated within the Tularosa Basin of the Rio Grande Rift between the San Andres and Sacramento Mountains in southern New Mexico, is the largest (~ 500 km^2) known field of gypsum dunes globally (Fig. 1). The field consists of a core of crescentic dunes flanked to the north, east and south by fields of parabolic dunes (Fig. 2). The field ends abruptly at Alkali Flat, an extensive, largely deflationary gypsum plain, which is flanked westward by active playas with precipitation of gypsum and minor amounts of other evaporites. Lake Lucero is the largest of these playas, which occupy the topographically lowest area of the basin. The entire complex rests upon accumulations of pluvial Lake Otero, which extended across the width of the basin during the Late Pleistocene (Herrick, 1904; Kottlowski, 1958; Seager et al., 1987). Gypsum is largely derived from leaching of evaporite-rich Permian strata flanking the basin (Allmendinger, 1972). The dune sand is derived through deflation of evaporite beds of Lake Otero and the younger playa lakes.

The dune field has been addressed in numerous studies (see summary in Langford, 2003), the modern era of which was initiated by McKee (1966). Fryberger (2000) provides an extensive overview of the dune field and its regional context. Most recently, Langford
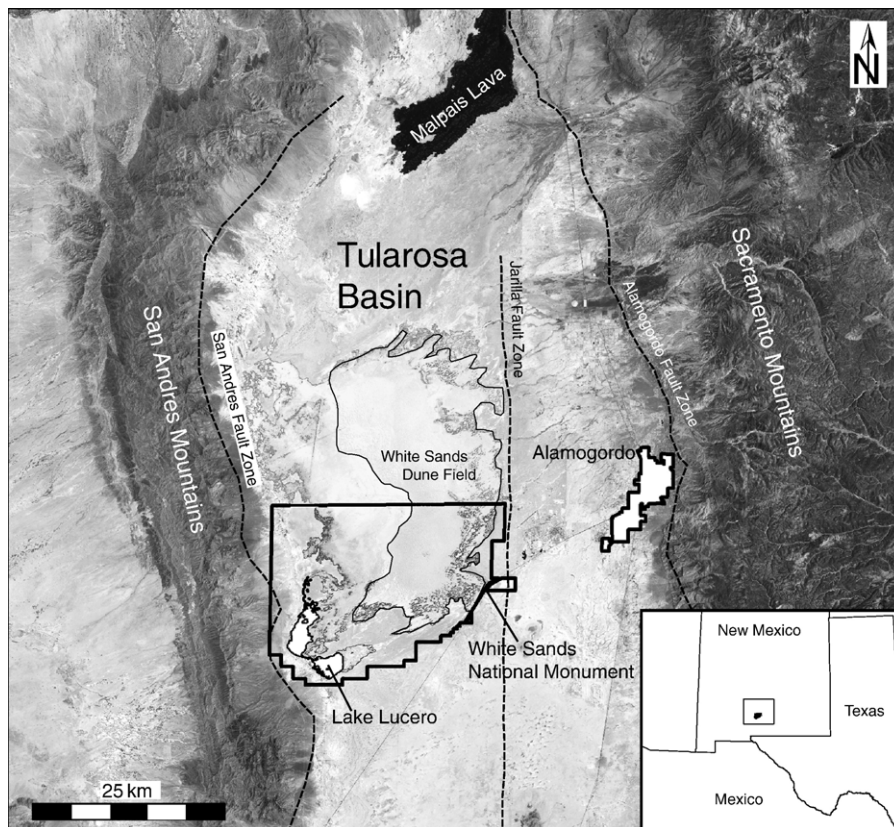

Fig. 1. Location of the White Sands Dune Field within the fault-bounded Tularosa Basin in southern New Mexico. The Tularosa Basin is within the much larger Rio Grande Rift. The southern portion of the dune field is within the White Sands National Monument. Note modern playa Lake Lucero within the SW corner of the Monument.

Fig. 2. White Sands Dune Field, showing a core of crescentic dunes rimmed by parabolic dunes, yielding westward to Alkali Flat, and then a zone of active playas, including Lake Lucero. Zonation from Fryberger (2000). Note the contemporary flux of aeolian gypsum from Lake Lucero, giving rise to parabolic dunes. White Sands National Monument headquarters (HQ) shown with road culminating in the "Heart of the Dunes Loop". Paleo-shorelines L1, L2, Lake Lucero shoreline, and one shoreline from Lake Otero (elevation of 1210 m) from Langford (2003). Positions of monitored dune (D-1), core (UT-1), trench (T-1) shown, along with previous cores from McKee and Moiola (1975) (MM-1 → MM-4), Park Service wells (PS-1, PS-2, PS-6), and trenchs from Simpson and Loope (1985) (SL-1, SL-2). Note position of cross-section A–A′ shown in Fig. 3.

(2003), through the documentation of paleo-shorelines and building upon a hypothesis introduced by Fryberger (2000, his Figs. 2–6), proposed that the dune field initiated during a specific constructional event triggered by basinal deflation and aeolian sand generation asso-ciated with regional aridity at ∼7000 yr. This view is contrary to thinking that the dunes originated through progressive, continuous deflation of the gypsum flat (e.g., McKee and Moiola, 1975), but in agreement with recent works that show dune fields commonly

correspond to specific constructional events associated with climatic change, the development of a sediment supply, or changes in the wind regime (e.g., Kocurek, 1998; Lancaster et al., 2002; Beveridge et al., in press).

The purpose of this paper is three-fold. First, we report ages obtained by optically stimulated luminescence (OSL) from a core that penetrated through the dune-field accumulation. These dates serve both as a test of the age of the field as proposed by Langford (2003), and allow estimates of the overall rate of accumulation within the dune field. Second, we address the nature of recent dune and interdune area dynamics via monitoring, and the character of their accumulations via natural exposures and trenches. Third, recent rates of accumulation as determined from the trenches are compared to the long-term accumulation rate within the field as determined from the core.

2. Methods

Coring was preformed adjacent to the "Heart of the Dunes Loop" at an elevation of 1216 m using the Texas Bureau of Economic Geology truck-mounted rotary drill with an inner 7.6 cm in diameter, pre-slit PVC coring tube in 75 cm long segments (UT-1 in Fig. 2). The core segments were split within a dark trailer, with half the core retained for study and the other half sampled for OSL dating.

OSL dating was done on quartz grains, which account for a few percent of all the core samples. The extraction of quartz from the gypsum sand was non-trivial. The samples were first treated with H_2O_2 to remove any organic matter. The residual fraction was treated either with ethylene diamine tetra acetic acid (EDTA) followed by floatation, or gypsum was simply dissolved in warm, concentrated 12 N HCl for extended durations ($\sim$ 3 h). Quartz grains in size range of 90–150 µm (samples 1–5) and 75–110 µm (samples 6 and basal clay) were obtained by sieving and etched for 40 min in 40% hydrofluoric acid followed by 12 N HCl treatment. Sample grains were loaded onto a stainless steel (9.5 mm diameter) disc. Measurements were made using an upgraded version of Riso automated TL/OSL system TL-DA-12 modified with blue light stimulation LEDs. The samples were stimulated by Blue LEDs with a peak wavelength at 470 nm (power 50 mW/cm^2) and the Blue Light Stimulated Luminescence (BLSL) was measured through a filter combination of a U-340 and Schott BG-39. The dose rate from natural radiation was low, making cosmic rays a dominant contributor. A depth-modified cosmic ray dose was used. The cosmic ray dose rate was computed for the site using the method of Prescot and Hutton (1994). The external dose rate was measured using alpha counting (uranium and thorium) and gamma counting (for potassium estimation). Equivalent doses were determined for each sample using BLSL measurement and the conventional single aliquot regeneration (SAR) method (Murray and Wintle, 2000). The dose rate computation assumed an equilibrium in the decay series and this aspect is being tested further. In the case of the series being in disequilibrium, the ages will be minimum estimates. In the series, with the exception of the two basal samples, the cosmic ray dose ranged from 40–80%, implying that the age offset as a result of any possible disequilibrium is likely to be small. The water content was measured in the laboratory from sealed field samples.

A sinuous crescentic dune (D-1 in Fig. 2) was monitored and surveyed over a 1 yr period in order to document dune response to each significant wind direction. Dune response in terms of surface processes was then compared to a longer term record of the dune as revealed in a plan view of its cross-strata.

Trenches were excavated with a backhoe across three interdune areas and the basal portions of their associated dunes along a transect oriented N60E, or perpendicular to the local dune crestal trend (T-1 in Fig. 2). This transect is one of two that had been previously surveyed, approximately every three months, over a 2.5 yr period using an Elta 4 electronic tacheometer in order to monitor dune migration rates and changes in dune morphology (Crabaugh, 1994). Trench depth was limited by the water table, and ranged from 0.2 to 1.5 m. Trenches were cleaned, photographed, surveyed and drawn in detail for a total of 188 m over a total transect distance of 470 m.

3. Dynamics and age of dune-field emplacement

3.1. Geomorphic and stratigraphic position

As shown by Langford (2003), a consideration of the elevations of outcrops of Lake Otero strata and the playa shorelines on Alkali Flat are critical to understanding emplacement of the White Sands Dune Field. Seager et al. (1987) identified late Pleistocene lacustrine gypsiferous basin-floor deposits at elevations as high as 1218 m., and deposits of Lake Otero are noted by Langford (2003) in erosional gullies at elevations below 1215 m. Lake Otero deposits are distinct from the overlying accumulation of gypsum, and consist of laminated clays and silts, gypsiferous marls, limestone and massive silts containing large gypsum crystals (Langford, 2003).

Erosional shorelines cut into sediment accumulations of Lake Otero identified by Langford (2003) on Alkali Flat consist of: (1) a shoreline rimming Lake Lucero with the playa floor at 1185 m, (2) the L2 shoreline at 1191 m, and (3) the L1 shoreline at ∼1200 m in elevation (Figs. 2 and 3). The active dune field begins above the L1 shoreline, with Alkali Flat extending at elevations below 1200 m.

The thickness of gypsum underlying the dune field and overlying deposits of Lake Otero has been measured at several drill sites, but mostly near the "Heart of the Dunes Loop" (Fig. 2). UT-1 penetrated 8.7 m of gypsum before striking a gypsiferous clay bed, which is interpreted as deposits of Lake Otero. Three nearby groundwater-monitor wells emplaced by the Park Service show depths to the clay layer as 7.2 m at PS-1, 8.2 m at PS-2, and 7.3 m at PS-6 (W. Conrod, per. comm., 2003). Four cores from McKee and Moiola (1975) show the dune-field accumulations as: MM-1: 10.4 m, MM-2: 9.3 m, MM-3: 9.4 m, and MM-4: 7.0 m.

Taking an average of 8.5 m of gypsum thickness, the elevation at the base of the gypsum accumulation near the south-central dune field is 1208 m. Using an elevation of 1215 m as the downwind pinchout of the accumulation against Lake Otero strata, and an upwind pinchout at an elevation of 1201 m just above L1, the lower bounding surface of the gypsum accumulation dips westward at about 0.09° (Fig. 3). The extent to which this surface is erosional or mimics the depositional slope of the Lake Otero beds is difficult to determine, but Langford (2003) interpreted the surface as the result of terminal Pleistocene deflation to the L1 shoreline and predating the dune field. The drop in elevation from the L1 shoreline to the L2 shoreline was interpreted to represent a second period of significant erosion with scour of Lake Otero beds by ∼9 m. A third period of deflation downcut to the Lake Lucero floor with removal of an additional 6 m of strata (Langford, 2003).

3.2. Model of dune-field emplacement

Langford (2003) postulated that the dune field originated in response to the L1 to L2 deflationary event, and that the sediment supply for the field was in large measure derived from scour of a gypsum layer at 1194 m in elevation, first described by Allmendinger (1972). The sediment supply was enhanced during a second period of deflation that downcut from the L2 shoreline to the Lake Lucero surface.

In this model, dune-field construction was in response to the creation of a sediment supply, which was the product of deflationary events that resulted from periods of aridity and a fall in the water table. Lake Lucero and other modern active evaporite-precipitating playas occupy the lowest portions of the deflated basin, incised into Lake Otero sediments. As evident from Fig. 2, gypsum aeolian sediment is derived from modern Lake Lucero, and it is reasonable to believe that earlier playas (i.e., playas represented by the L2 and L1 shorelines) also provided contemporaneous influx to the dune field. Modern precipitation of gypsum occurs on Alkali Flat as well, with a slow rate of deflation from the flat and sediment influx to the dune field.

Based upon archeological evidence associated with the shorelines, ^{14}C dates from a shoreline similar to L2 and Lake Lucero, and regional episodes of hydrologic change associated with increased aridity, Langford (2003) reasoned that basin deflation from L1 to L2 and initiation of the dune field occurred at ∼7000 yr, and deflation from L2 to the Lake Lucero surface was at ∼4000 yr.

3.3. OSL dates from core UT1

OSL dates and relevant data for samples taken from the core are given in Table 1. OSL samples 1, 2 and 3 were obtained from drill site 1, but this hole was
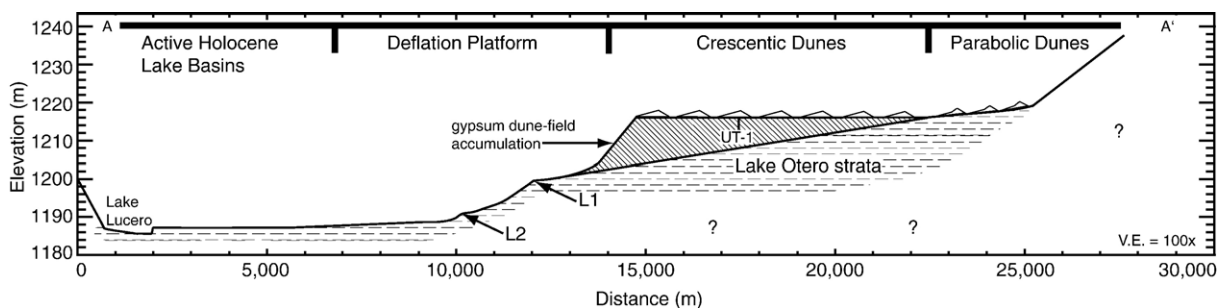

Fig. 3. Cross-section A–A′, as located on Fig. 2, showing a deflationary basin progressively downcut into Lake Otero strata. The dune-field gypsum accumulation is shown pinching out at an elevation of 1215 m against strata from Lake Otero, and tapering to zero above the L1 shoreline. Thickness at UT-1 is 8.7 m. Note that vertical exaggeration is 100×. Drawing inspired from Langford (2003, his Fig. 4).

Table 1
Summary of OSL data for samples taken at 1 m increments in core UT-1

Sample	Depth (m)	U (ppm)	Th (ppm)	K (%)	CR (Gy/ka)	Water (%)	D_e (Gy)	Dose rate (Gy/ka)	Age (ka)
Surface	0.25	0.42±0.03	0.11±0.13	0.020±0.001	0.232±0.023	18±4	0.10±0.01	0.30±0.01	0.3±0.04
1	1	0.05±0.04	0.21±0.15	0.021±0.002	0.197±0.019	5±1	0.50±0.03	0.24±0.02	2.1±0.2
2	2	0.13±0.00	0.00±0.00	0.020±0.002	0.168±0.016	14±3	0.70±0.06	0.22±0.02	3.2±0.2
3	3	0.20±0.01	0.07±0.07	0.042±0.011	0.145±0.014	13±3	0.80±0.06	0.22±0.02	3.6±0.3
4	4	0.30±0.10	0.06±0.06	0.050±0.013	0.126±0.012	13±3	1.00±0.01	0.23±0.02	4.3±0.4
5	5	0.12±0.04	0.29±0.14	0.101±0.030	0.103±0.010	9±2	1.10±0.08	0.25±0.02	4.3±0.3
6	6	1.49±0.10	0.20±0.38	0.101±0.031	0.097±0.009	13±3	3.01±0.28	0.58±0.10	5.2±0.4
Basal clay	9	1.12±0.07	0.29±0.27	0.220±0.102	0.068±0.007	20±5	4.10±0.30	0.56±0.10	7.3±0.5

abandoned at 3.75 m depth because of liquefaction and flowage into the hole after encountering the water table at 0.3 m in depth from the surface. Above the 3.75 m depth core recovery was nearly 100%, but only the upper 0.75 m had identifiable sedimentary structures. A second drill site, approximately 10 m from the first site, had about 50% core recovery for depths ≥ 4 m, and OSL samples 4, 5, 6 and from the basal clay layer (Lake Otero strata) were taken from this site. The basal clay bed has an OSL date of 7.3±0.5 ka. It is reasonable to presume that this uppermost bed of Lake Otero at the coring site does not represent the pre-erosional top of Lake Otero strata. The age obtained within the gypsum body at a depth of 6 m is 5.2±0.4 ka. Within the constraints of the OSL dates, therefore, Langford's (2003) conclusion that the dune field was initiated at ∼7000 yr is reasonable.

3.4. Sediment state

The dynamic interplay between climatic forcing, the sediment source, and the availability of this sediment for dune-field construction can be illustrated with the sediment state concept of Kocurek and Lancaster (1999), as shown in Fig. 4. The sediment supply was generated by gypsum precipitation in Lake Otero and subsequent playa lakes. A stepwise decrease in the production of a sediment supply is shown as the lakes contracted through time, but the detailed shape of this curve is unknown. Sediment deposited within the lakes was not available for aeolian transport until the water table fell, and was therefore stored (S) because its availability was limited (S_{AL}). With the onset of aridity, stored sediment was deflated and transported as lagged (in time) influx (LI). The rate of deflation was probably limited by the water table so that the influx was availability-limited (LI_{AL}). Contemporaneous influx (CI) from the active playas, as occurs with Lake Lucero today, is envisioned as occurring throughout the history of the dune field, probably enhanced by annual wet/dry cycles. The total sediment influx to the dune field,

therefore, has probably consisted of both lagged and contemporaneous influx that was availability-limited (CLI_{AL}). Although it is probable that the overall wind energy varied with climatic change, no definitive knowledge exists regarding the transport capacity of the wind over time, and this aspect of the sediment state is shown constant in Fig. 4.

4. Current dynamics of dunes and interdune areas

4.1. Overall system dynamics

The White Sand Dune Field is primarily a wet aeolian system in the terminology of Kocurek and Havholm (1994) in that the behavior (e.g., accumulation, bypass, erosion) over time of the accumulation surface is a function of the water table. The accumulation surface is taken as the surface connecting the interdune troughs (Rubin and Hunter, 1982; Kocurek and Havholm, 1994). Within the White Sands Dune Field, the capillary fringe of the water table is at or near the accumulation surface. In wet systems, accumulation occurs with a relative rise of the water table, whereas deflation occurs when the water table falls, and bypass occurs with a static water table. A particular aspect of wet aeolian systems is interdune accumulation. Aerodynamically, the interdune area downwind of the lee-slope separation cell and line of flow reattachment is at least potentially erosional because the wind in the newly formed boundary layer (originating at the line of reattachment) accelerates owing to the downward flux of momentum from overlying, higher speed flows (Frank and Kocurek, 1996). Whereas sand is typically deflated from interdune areas in dry aeolian systems, accumulation can occur within interdune areas of wet systems because moisture both fosters deposition and hinders erosion.

However, because of surface cementation by gypsum (e.g., Schenk and Fryberger, 1988), the system is in part also a stabilizing system in the terminology of Kocurek
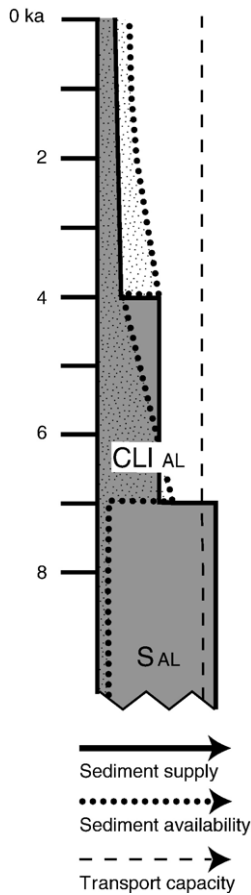
Fig. 4. Sediment state diagram for the White Sands Dune Field. Sediment supply, sediment availability and transport capacity of the wind are given as volumetric rates that are plotted against time. Sediment supply (shaded), generated by lacustrine gypsum deposition, is shown in stepwise constrictions at 7000 and 4000 yr in a progressive onset of aridity, and is availability-limited (S_{AL}) by the water table. Dune-field construction (stippled) occurs because of a fall of the water table with regional aridity that increases sediment availability, which is limited by the height of the water table. Aeolian influx to the dune field consists of both lagged influx (derived from deflation of the previously stored lacustrine sediment) and contemporaneous influx from playas (CLI_{AL}).

and Havholm (1994). Within stabilizing systems, factors such as vegetation, coarse lags or surface cementation control the behavior of the accumulation surface over time, such as accumulation occurring because of the presence of vegetation. At White Sands, surface cementation primarily acts to limit deflation. In one manifestation, deflating dune foresets commonly show a "corrugated" (term from Simpson and Loope, 1985) microtopography resulting from differential cementation. Using the aeolian stratification types identified by Hunter (1977a), the more tightly packed, better cemented wind-ripple laminae stand in relief, whereas the more loosely packed, less cemented grainflow strata (and to a lesser extent, grainfall strata) are hollows (see examples in Schenk and Fryberger, 1988). Corrugated surfaces and other manifestations of microtopography are common in ancient aeolian strata that are interpreted as representing damp or cemented surfaces (Kocurek, 1981; Havholm and Kocurek, 1994).

Groundwater flow within the Tularosa Basin is basinward through alluvial fans emanating from the San Andres and Sacramento Mountains, then axial southward with local discharge at Lake Lucero (Allmendinger and Titus, 1973). Within the dune field, the water table is perched owing to the contrast in permeability between the relatively porous dune-field accumulation and the underlying, less porous strata of Lake Otero. Crabaugh (1994, her Fig. 3.4) showed that the water table fluctuates seasonally in response to changes in precipitation and potential evaporation (Allmendinger, 1972), rising to its shallowest level during the winter months and sinking to its lowest level during the late summer. During the winter, interdune ponding in the "Heart of the Dunes Loop" area may occur as a result of runoff.

4.2. Crescentic dunes and wind regime

The crescentic dunes at White Sands range up to about 15 m in height, and occur as fairly continuous NNW-trending (345°) ridges that average 247 m in crest length with an average spacing of 136 m (Ewing et al., 2006). Fryberger (2000, his Fig. 2.17) shows a 060° wind resultant from nearby Holloman AFB (Fig. 5A). The dunes, therefore, are oriented borderline transverse (75°) to the resultant, using the classification of Hunter et al. (1983). This orientation indicates that the wind regime and resultant dune behavior are more complex than the crescentic dune shapes suggest and as typically portrayed (i.e., NE dune migration under dominant winds from the SW). The dominant winds from the SW (and W) are strongest during the winter–spring. Winds from the N–NW occur during the fall and winter, and winds from the S–SE occur during the spring–summer.

4.3. Monitored dune

Fig. 5B–F show the monitored dune during the significant wind directions. The dunes are oriented most transverse to the SW winds, maximum sand transport and dune migration occurs during these winds (Crabaugh, 1994), and the dunes are characterized by sharp brinks and slipfaces dominated by grainflow/grainfall processes (Fig. 5B). Wind ripples on the lee face are restricted to areas of curvature between concave- and
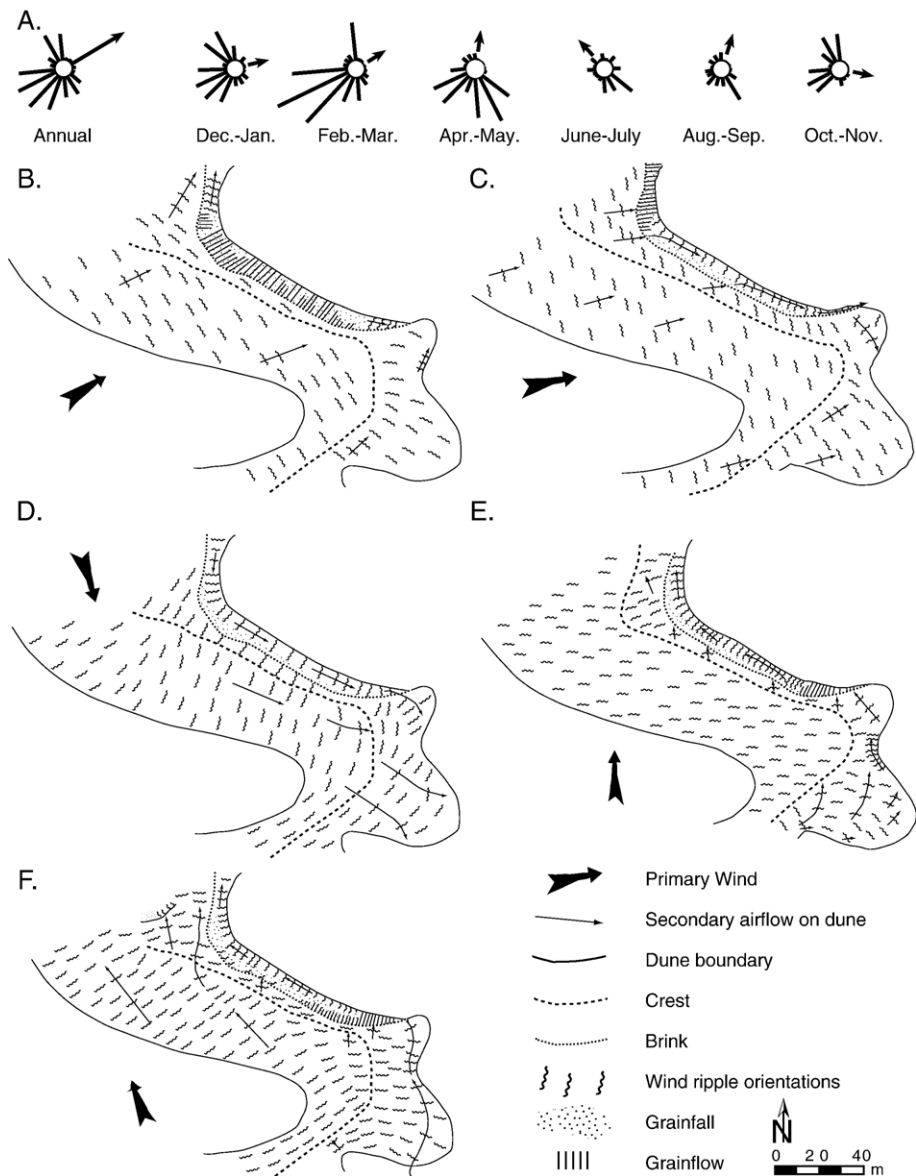
Fig. 5. (A) Wind regime from Holloman AFB (from Fryberger, 2000). (B)–(E). Primary wind and secondary airflow with surface processes on the monitored dune during the major wind directions. Note that winds from the SW are most transverse to the dune and result in a slipface marked by grainfall/grainflow processes (B). Winds from the W and NNW result in deflected lee airflow to the SE and lee wind ripples (C–D). Winds from the S and SE result in a reversal of this secondary airflow on the lee (E–F).

convex-downwind segments where the wind incidence angle is oblique. Winds from the W, however, strike the dunes obliquely, resulting in deflected alongslope air flow on the lee face and predominantly wind ripples migrating to the SE (Fig. 5C). A similar pattern of lee face ripples occurs with winds from the NNW (Fig. 5D). Winds from the N–NW also result in rounding of dune brinks and crests, minimal crest-normal migration, and lee face reactivation (Crabaugh, 1994). A reversal in the direction the deflected alongslope transport occurs with

winds from the S–SE (Fig. 5E–F). In the monitored dune, grainfall/grainflow processes are largely restricted to the concave-downwind portion of the dune where the incidence angle is high, whereas most of the lee face is dominated by grainfall transitional downslope into wind ripples migrating to the NW.

During her 2.5 yr monitoring period, Crabaugh (1994) showed dune migration rates to average 1.6 m/yr. During a nearly 6 yr monitoring period, McKee and Douglass (1971) documented barchan and crescentic
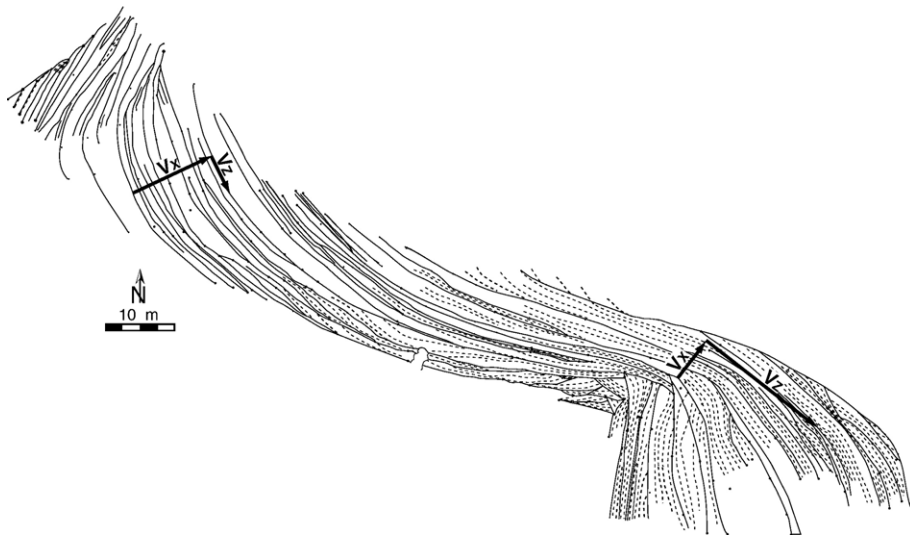
Fig. 6. Horizontal section of cross-strata reveal in the upwind eroded foresets of the monitored dune (Fig. 5). Solid lines were more prominent on the outcrop and largely represent reactivation surfaces; dashed lines represent foresets. This longer-term record of migration of the monitored dune shows both crest-normal (V_x) and along-crest (V_z) components of migration, as determined by the shifting positions of the centers of the concave- and convex-downwind portions of dune sinuosity. Note the ziz-zag structure developed along the convex segment of the dune.

dune migration rates of 1–4 m/yr. As revealed in the plan-view section of the monitored dune, however, this crest-normal component of migration (V_x) is accompanied by an along-crest migration (V_z) of the dune sinuosity to the SE (Fig. 6). The convex-downwind segment shows a zigzag structure formed by scour of the NW side of the convexity prior to deposition of a new subset of cross-strata. Crest-normal migration corresponds to the dominant winds from the SW, whereas oblique wind components from the N–NW (and to a lesser extent, winds from the W) induce the along-crest migration, and reshaping of the convex-downwind segment. Winds from the S–SE are a lesser component of the wind regime (Fig. 5A), and apparently play a minimal role in defining the dune shape.

4.4. Interdune areas

The location for trench T-1 was selected because of the range of interdune aspects exhibited, which are typical of interdune areas within the White Sands Dune Field (Fig. 7). In terms of interdune shape, Segment 1 of T-1 consists of a streamwise broad interdune flat, whereas Segment 3 consists of a relatively small, enclosed interdune depression, and Segment 2 shows an intermediate shape with aspects of both end members.
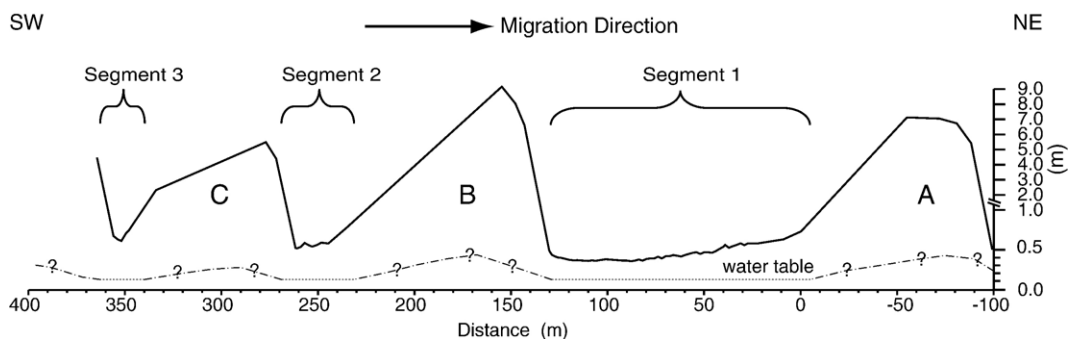

Fig. 7. Surveyed transect and location of trenches (Segments 1–3 in Fig. 9A–C). Note the depth of scour of the interdune floors increases with interdune streamwise length. Position of the water table beneath the trenched segments shown; shape of the water table beneath the dunes is unknown, but may rise with dune topography. The capillary fringe extended to the surface in Segments 1–2, but was below the surface in Segment 3. Modified from Crabaugh (1994).

Fig. 8. Interdune flat (Segment 1 in Fig. 7) showing stoss slope of the downwind dune yielding upwind to differentially eroded foresets of this dune, which are progressively buried by wet/damp interdune deposits. The figure illustrates the surface manifestation of climbing dunes and interdune areas. Migration of the dune and interdune area, with net deposition (i.e., accumulation) generates time-transgressive layers (i.e., translatent strata).

The depth of scour of the interdune floors closely relates to the size of the interdune areas, such that the broad interdune area (Segment 1) is scoured down to the capillary fringe of the water table, whereas the capillary fringe is well below the floor of the enclosed depression (Segment 3).

In turn, depth of scour controls the nature of interdune deposition. Wind ripples extend from the basal apron of the upwind dune, across the interdune depression, and to the stoss slope of the downwind dune in Segment 3 (i.e., dry interdune surface in terminology of Kocurek, 1981). In contrast, Segments 1–2 show the rippled stoss slope of the downwind dune yielding upwind to differentially eroded foresets of these dunes, and the eroded foresets are then progressively buried in the upwind direction by flat-bedded, wet–damp surface interdune deposits (Fig. 8).

Wet–damp surface interdune deposits at White Sands have been described by Fryberger et al. (1988), and consist predominantly of salt ridges (see Fryberger et al., 1984). These features form along surfaces within the capillary fringe where gypsum precipitates, and are accompanied by the growth of mats of microorganisms and algae. Salt ridges display a characteristic surface of wrinkles and pustules, and laminated strata with small-scale contortions in cross-section. Typically during the late fall through early spring, interdune floors are at their dampest and deposition occurs by sediment trapping by mat growth and rise of the capillary fringe. Conversely, during the late spring through early fall when the interdune surfaces are at their driest, the salt ridges and associated mats are typically dry, brittle with an admixture of wind-blown sand.

5. Nature of accumulations revealed by trenches

5.1. Overall strata geometry

In the trench across Segment 1, the active (i.e., wind ripples overlying truncated lee foresets) stoss slope (0–9 m in Fig. 9A-1) of Dune A yields to eroded foresets (9–29 m in Fig. 9A-1), which are then onlapped and irregularly infilled by interdune accumulations (29–48 m in Fig. 9A-1–2). From this point upwind, foresets are completely buried beneath interdune strata. Dune A, which has a crestal height of 7 m, is represented as a set 65 cm thick at the 9 m marker, 35 cm thick at the 29 m marker, and continues to thin but remains as a traceable set to the 97 m marker. From this point to the 128 m marker, only a prominent surface separates accumulations of the modern interdune area from the older interdune accumulations that underlie Dune A (Fig. 9A-3). Trench depth is filled with thickening interdune strata (up to 30 cm) deposited within the current interdune area for the remaining trench length.

In the trench across Segment 2, the active stoss slope (0–2 m in Fig. 9B) of Dune B yields to eroding foresets (2–14 m in Fig. 9B), and then to sporadic modern interdune infill (14–24 m in Fig. 9B), and finally to progressive burial by a thickening wedge (up to 20 cm) of interdune accumulations until these are buried beneath
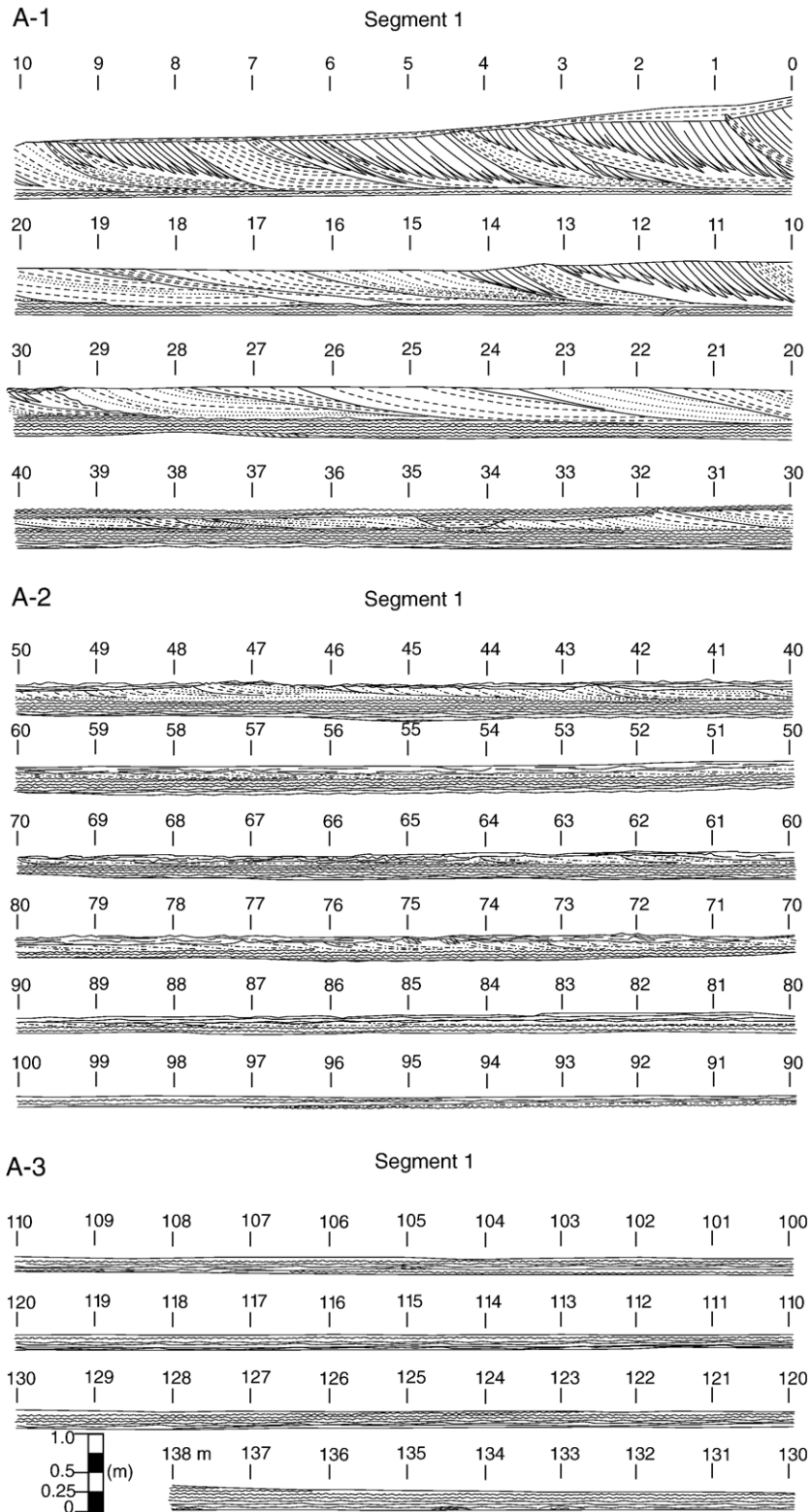
Fig. 9. Drawings from the field of trenches shown in Fig. 7. (A1–3) Segment 1, (B) Segment 2, (C) Segment 3. See text for detailed descriptions and discussion. There is no vertical exaggeration in these diagrams. From Crabaugh (1994).
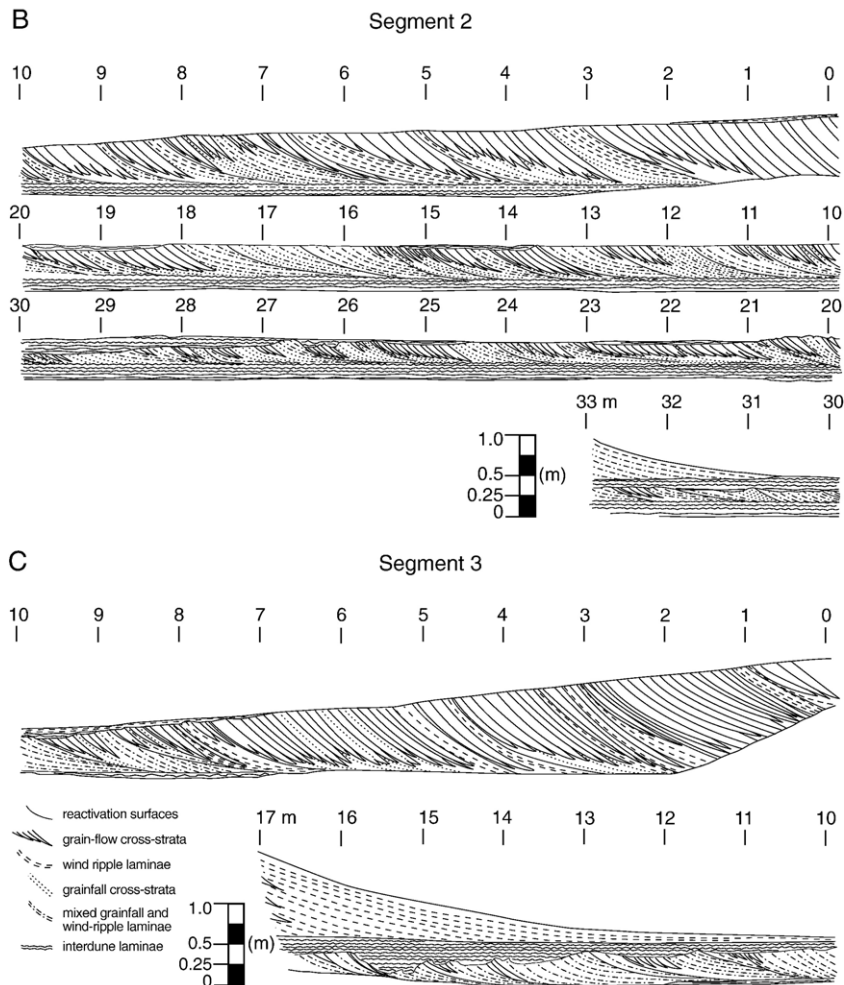
Fig. 9 (*continued*).

the lee apron of Dune C (24–33 m in Fig. 9B). Dune B, with a crestal height of 8.75 m, is represented by a 40 cm thick set at the 18 m marker, 25 cm at the 24 m marker where complete burial of the set begins, and is only about 15 cm thick at the 33 m marker where it is buried by both interdune accumulations and the prograding lee slope of Dune C. Unlike in Segment 1, there is no amalgamation of the interdune accumulations above and below the set of cross-strata representing Dune B.

In the trench across Segment 3, eroded foresets on the stoss slope of Dune C are onlapped by the wind-rippled apron of the next dune upwind at the 7 m marker in Fig. 9C. However, the trench shows that this rippled lee apron is underlain by wet–damp interdune accumulations. These onlap the set of cross-strata representing Dune C at the 9 m marker in Fig. 9C, and form a thickening wedge of interdune strata that overlie foresets showing marked differential erosion. At the last point

where the base of the set deposited by Dune C (with a crestal height of 4.5 m) was reached in the trench (12 m marker in Fig. 9C), the set is up to 40 cm thick.

5.2. Interpretation of strata geometry

The strata revealed by the trenches is consistent and in continuity with the surface expression of the dunes and interdune areas (Fig. 8). Dunes are clearly not just migrating over the accumulation surface (i.e., bypassing), but rather are leaving sets of cross-strata that are irregularly, but progressively buried beneath interdune deposits, which are, in turn, buried beneath the prograding lee of the next upwind dune. Although dunes along the transect were not trenched so that the trenches could be physically connected, a reasonable extrapolation of the dune and interdune strata exposed in the trenches is their continuity under the dunes (Fig. 10). In the terminology
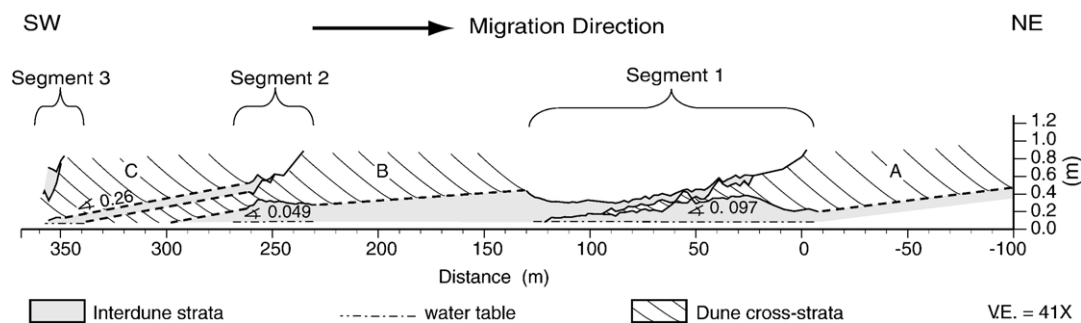
Fig. 10. Interpretation of transect shown in Fig. 7 constructed by extending the strata shown in the trenches (Fig. 9) under the dunes, which were not trenched. Angles of climb shown are measured with respect to the horizontal water table as evident in the trenches. Modified from Crabaugh (1994).

of Allen (1970), Hunter (1977b), Rubin and Hunter (1982) and Kocurek and Havholm (1994), the trenches (Fig. 9) and their extrapolation (Fig. 10) show climb in which the dune sets and interdune strata are migrating, time-transgressive translatent strata that rise with respect to the accumulation surface. Bedform climb is obviously subcritical (terminology of Hunter, 1977b), with an overall positive, but fluctuating angle of climb in which there are times of bypass (zero angle of climb) and net deflation (negative angle of climb) (see examples in Rubin, 1987).

The net angle of climb θ, as measured from the accumulation surface and with respect to the interdune surface (see Kocurek, 1996), is defined by the tan $\theta = V_y / V_x$, where V_y is translation rise over a migration distance of V_x (Allen, 1970). The local accumulation surface dips in the migration direction at about 0.04° (Fig. 7), yielding angles of climb of 0.137° for Dune A, 0.089° for Dune B, and 0.3° for Dune C, with an average of 0.18°. Depth to the water table in the trenches, which defines the *potential* accumulation surface in a wet system, shows that the water table is horizontal beneath the interdune areas (Fig. 7). Measured from the horizontal, the angles of climb are 0.097° for Dune A, 0.049° for Dune B, and 0.26° for Dune C, yielding an average of 0.14° (Fig. 10).

Consistent with the observation that the depth of deflation of the interdune areas increases as the streamwise length of the interdune area increases (Fig. 7), Segment 1 shows complete upwind truncation of the set deposited by Dune A, whereas the sets from Dunes B and C continue entirely across their upwind interdune areas. For all sets, set thickness roughly decreases as interdune area streamwise length increases. In one interpretation, the sets simply thin toward their points of origin, but it seems unlikely that these dunes originated in the central field. The more likely interpretation is that the interdune surfaces are periodically deflated (e.g., dry years when the water table falls).

Once exposed in the interdune area as the dune migrates, a set of cross-strata can only remain a constant thickness or be thinned by erosion; the greater the streamwise length of the interdune area (given relatively constant dune migration rates), the longer the interdune area remains as an exposed surface and the greater the probability that deflationary dry years will occur. This characteristic is most likely associated with wet aeolian systems where the water table fluctuates as part of a climatic cycle, and would be less prevalent where the relative height of the water table is a function of other parameters such as changes in sea level or subsidence (e.g., Kocurek and Havholm, 1994; Kocurek et al., 2001).

Correspondingly, the thickness of the interdune deposits increases as interdune streamwise length increases, and increases overall in the upwind direction. Maximum interdune accumulation, as reached just downwind of the lee of the next upwind dune, is 30 cm in Segment 1, 20 cm in Segment 2, and about 15 cm in Segment 3, although thicker deposits occur in the severely eroded hollows on the set representing Dune C in Segment 3. Unlike dune strata that can only remain constant in thickness or be deflated in an exposed interdune area, interdune depositional thickness can also increase. Given net deposition (i.e., a relative net rise in the water table over time such that accumulation occurs), the probability of increased interdune wet/damp surface accumulation should increase with increasing interdune streamwise length.

In a pioneer application of the of the concept of bedform climb, McKee and Moiola (1975, their Fig. 8) interpreted core data (MM-1 → MM-4 in Fig. 2) as the result of climb, but clearly grossly over-estimated the thickness of the translatent strata left by each migrating dune and interdune area, and consequently the angle of climb. Judging by the tendency for liquefaction of the gypsum deposits below the water table and the poor

retention of sedimentary structures within cores, one explanation of the results presented by McKee and Moiola (1975, their Fig. 9) is that layers grouped as deposits from single dune and interdune areas actually contain multiple such horizons.

Simpson and Loope (1985) recognized the problems in the McKee and Moiola (1975) interpretation in comparison to their trenches (SL-1, SL-2 in Fig. 2), which are similar to our trenches although they report a much greater degree of interdune amalgamation (see Figs. 6–7 in Simpson and Loope, 1985) than evident in our trenches (only from the 97–128 m markers in Segment 1, Fig. 9A). A relative rise in the water table within a field of dunes and interdune areas will cause a similar thickness of accumulation of both dune and interdune deposits, providing there is a similar capillary rise (Kocurek, 1996). As argued above, however, with a net low angle of climb in a wet aeolian system where there are periodic drops in the water table, the angle of climb will fluctuate from positive to zero and negative, with a bias toward removal of dune cross-strata. This dynamic process provides one cause of variations in scour depth within the overall concept of climbing bedforms.

5.3. Dune cross-strata

Sets of cross-strata exposed in the trenches show a consistent bundling of foresets separated by bounding surfaces (Fig. 9). Foresets can be distinguished by stratification types as grainflow, grainfall and wind-ripple laminae, allowing for the recognition of repetitive patterns. In the thickest preserved sets, the most common pattern is one in which the erosional bounding surface is conformably overlain by tangential foreset-to-toeset wind-ripple laminae, which yield to downlapping grainflow (commonly with basal grainfall) cross-strata that are truncated by the next bounding surface in the transport direction (Fig. 11). The second most common pattern shows the eroded bounding surface downlapped by grainflow cross-strata (with or without the tangential wind-ripple unit), which yield in the transport direction to wind-ripple laminae that are truncated by the next bounding surface. Other packages between bounding surfaces consist (1) entirely of wind-ripple laminae, and (2) a mix of grainfall and wind-ripple laminae. As set thickness decreases, tangential wind-ripple foresets dominate owing to truncation of the set at progressively lower levels. Erosional bounding surfaces occur on average every 1.4 m (with a range from ∼0.5 to 2.5 m) throughout all three trenches (Fig. 9).

In other aspects the sets are consistent with their surface expression. The upper surfaces of the sets (i.e., interdune surface in terminology of Kocurek, 1996) maintain their surface corrugated appearance with burial, and isolated occurrences of interdune strata (e.g., markers 14–15, 21–23, 25–26 in Segment 2, Fig. 9B) commonly lie within deflated hollows developed along sections of grainflow cross-strata (Fig. 11). The basal bounding surface of the sets is
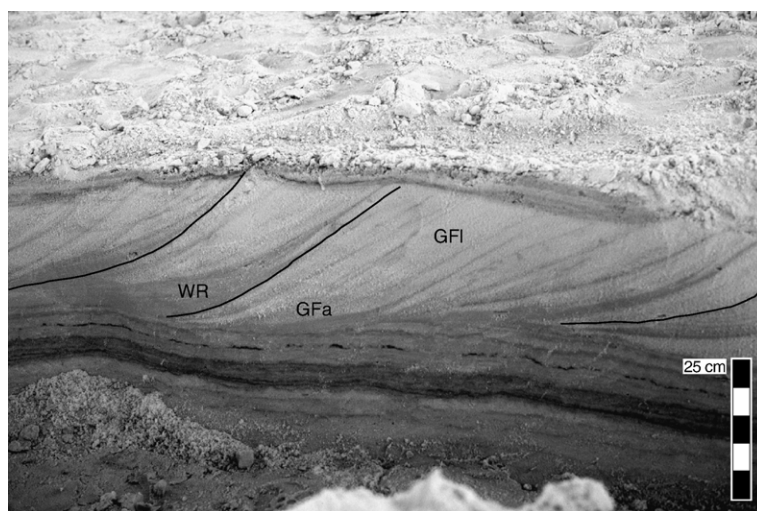

Fig. 11. Cyclic cross-strata as seen in trench cross-section (Segment 2). The pattern of downlapping grainflow cross-strata (GFl) commonly yielding downward to grainfall laminae (GFa) is interpreted to represent slipface progradation under transverse winds from the SW. Bundles of grainflow/grainfall cross-strata are punctuated by reactivation surfaces (lines) overlain by wind-ripple laminae (WR), interpreted to represent the onset of oblique winds from the NW–N. Note corrugated interdune surface truncating the set, with interdune infill in hollow. Older interdune strata underlie the set. Both interdune horizons show the characteristic light/dark laminae couplets.

relatively regular, reflecting only the salt-ridge topography of the interdune floor.

5.4. Interpretation of dune cross-strata

The spacing of bounding surfaces within the sets (1.4 m) is consistent with their measured migration rates (1.6 m/yr, see above), and the surfaces are interpreted as annual reactivation surfaces, with the repetitive patterns of cross-strata representing both annual cycles (see Hunter and Rubin, 1983) and position on the dune. Trenches by McKee (1966, his Fig. 7) show similar reactivation surfaces, which he interpreted to result from winter shifts in the wind direction.

Considered in detail, and in agreement with the monitored dune, grainflow cross-strata, representing transverse wind conditions, result from progradation of the slipface with the predominant winds from the SW. Grainflow strata are then truncated with development of reactivation surfaces with the onset of N–NW winds during the late fall and winter. These same winds give rise to wind-ripple laminae overlying the reactivation surface, reflecting the oblique nature of the wind incidence angle to the dune crestline. The pattern in which grainflow cross-strata yield to wind-ripple laminae that are then truncated may reflect (1) the transition to more oblique winds, or (2) position along the crestline. As seen in the longest trench (Segment 1, Fig. 9A), grainflow-dominated packages between reactivation surfaces (reflecting a transverse orientation), yield to wind-ripple-dominated packages upwind (reflecting an oblique to longitudinal orientation), as would be expected along a sinuous crestline if the sinuosity of the crestline migrated. As documented with the monitored dune, a southeastward migration of the crestline sinuosity is expected with the wind regime at White Sands.

5.5. Interdune strata

The laminae that compose the flat-bedded interdune accumulations within the trenches (shown schematically in Fig. 9) are thin (±1 cm) and relatively continuous (some traced for tens of metres), except for those occurring within isolated erosional hollows scoured into the cross-strata. The increased thickness of the interdune strata in an upwind direction, as described above, occurs primarily because of an increased number of laminae (Fig. 12), although the laminae themselves also tend to thicken somewhat in the upwind direction. Well-preserved individual laminae show a distinct alternation that is typically gradational upward. Relatively clean, white sands yield upward to a band of dark, organic-
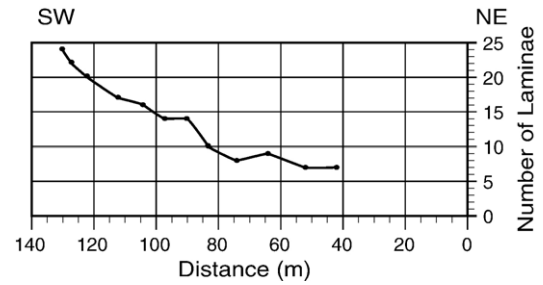

Fig. 12. Count of the number of laminae (dark/light couplets) at distances across the interdune area (Segment 1) shown in Fig. 9A. From Crabaugh (1994).

rich, commonly crinkly sand (Fig. 13). In a vertical section through an entire interdune accumulation, the concentration of organic-rich laminae increases upward.

5.6. Interpretation of interdune strata

The interdune accumulations appear to reflect deposition on the modern interdune areas in which sand is blown onto the surface and incorporated into the seasonal cycle of the salt ridges and algal/organic mats. The banding of laminae is interpreted to correspond to seasonal wetting with a rise of the capillary fringe through wind-blown sand, sand trapped by adhesion onto the damp surface, and culminating in development of the algal/organic mats during periods of maximum wetness. The increase in the number of laminae upwind reflects the increasing time that the interdune surface has been an exposed surface, whereas the thickening of the laminae upwind and the increase in the organic content vertically reflects relatively lateral passage of the interdune area into lower and wetter areas with dune migration.

Because the light and dark banding is seasonal in origin, the laminae are interpreted as interdune varves. If their preservation is complete, the number of varves (one light and dark couplet) should correspond to the dune migration rate. Twenty-four light/dark couplets are present at the maximum upwind position (138 m marker in Fig. 9A-3) of interdune Segment 1 (Fig. 12). Where interdune accumulation within this interdune started in the past is unknown, but assuming it began where it did at the time of the trenching (the 30 m marker in Fig. 9A-1), then the dunes would be migrating at 4.5 m/yr (i.e., 108 m/24 yr). This rate is considerably faster than the dune migration rate determined from the spacing of the annual reactivation surface (1.4 m/yr) or from the monitored rate (1.6 m/yr). A shortening of the length over which interdune accumulation occurred to 36 m is required to account for the 24 varves to represent a
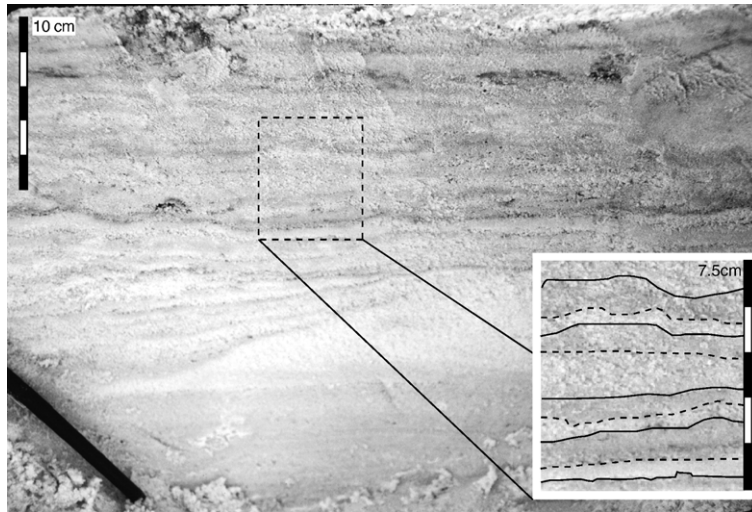
Fig. 13. Interdune light and dark laminae couplets, with enlargement, interpreted as annual varves, as seen in trench cross-section from Segment 1. Dark laminae are thought to represent algal/organic mats that develop during the wet portion of the year, whereas the light laminae reflect wind-blown sand deposited during drier portions of the year. Note the onlap of interdune laminae onto dune microtopography at the base of the section.

complete record at an average dune migration rate of 1.5 m/yr (i.e., 1.5 m/yr×24 yr). The most likely explanation, and one in agreement with our conclusion regarding the upwind thinning of the sets of cross-strata in the trenches, is that the interdune varve record is incomplete owing to periodic scour during dry periods. Using the streamwise length of the interdune area currently showing accumulation (108 m) and the average dune migration rate of 1.5 m/yr suggest that potentially 72 varve couplets could have been deposited. By this estimation, about 2/3 of the varves are not represented, having never been deposited or having been subsequently removed by deflation.

6. Dune-field accumulation

The OSL dates obtained from UT-1 afford the opportunity to determine the long-term accumulation rate within the dune field and to compare this rate to that determined from the climbing translatent strata exposed within the trenches. Taking 7 ka as the age of the dune field and the total thickness of the gypsum body near UT-1 as 8.5 m, yield an average accumulation rate of 1.2 mm/yr. The calculated cumulative accumulation rate ranges between 1.2–1.7 mm/yr (Fig. 14). Calculated by increments of depth, accumulation rates range from 0.5–2.5 mm/yr (Fig. 14). The occurrence of the same age for OSL samples at depths of 4 m and 5 m probably resulted from liquefaction and flowage within the drill hole. The calculated accumulation rate based upon the climbing strata within the trenches can be determined

from the relationship $\tan \theta = V_y / V_x$, in which 0.14° as the angle of climb (θ) and the average dune migration rate (V_x) is 1.4 m/yr, yielding an average accumulation rate (V_y) of 3.4 mm/yr. This rate of accumulation over 7000 yr would yield a section thickness of nearly 24 m. As is often the case, the short-term accumulation rate is significantly greater than the long-term rate.

Compaction can be expected to account for some section shortening in comparing the accumulation rates calculated for the core versus that determined from the trenches. In addition, dissolution of gypsum may be an additional cause of section shortening. These factors, however, probably do not account for the total differences in the accumulation rates.

One explanation is that the accumulation rate has indeed varied significantly over time. For example, the highest rate of accumulation occurs between 3.2–3.6 ka, a period that follows the deflationary event at ∼4000 yr speculated by Langford (2003) as the period of deflation from L2 to the Lake Lucero surface.

A second explanation is that accumulations have been removed. Deflation of accumulations could occur over short intervals of time (i.e., annual to decadal), essentially similar, but of a greater magnitude, to that deduced from the trenches in which both dune and interdune strata have been deflated. Alternatively, significant portions of section may have been removed, constituting unconformities in the geologic sense.

Overall, the area of the "Heart of the Dunes Loop" may have a higher rate of accumulation than in other portions of the dune field. The current drainage pattern
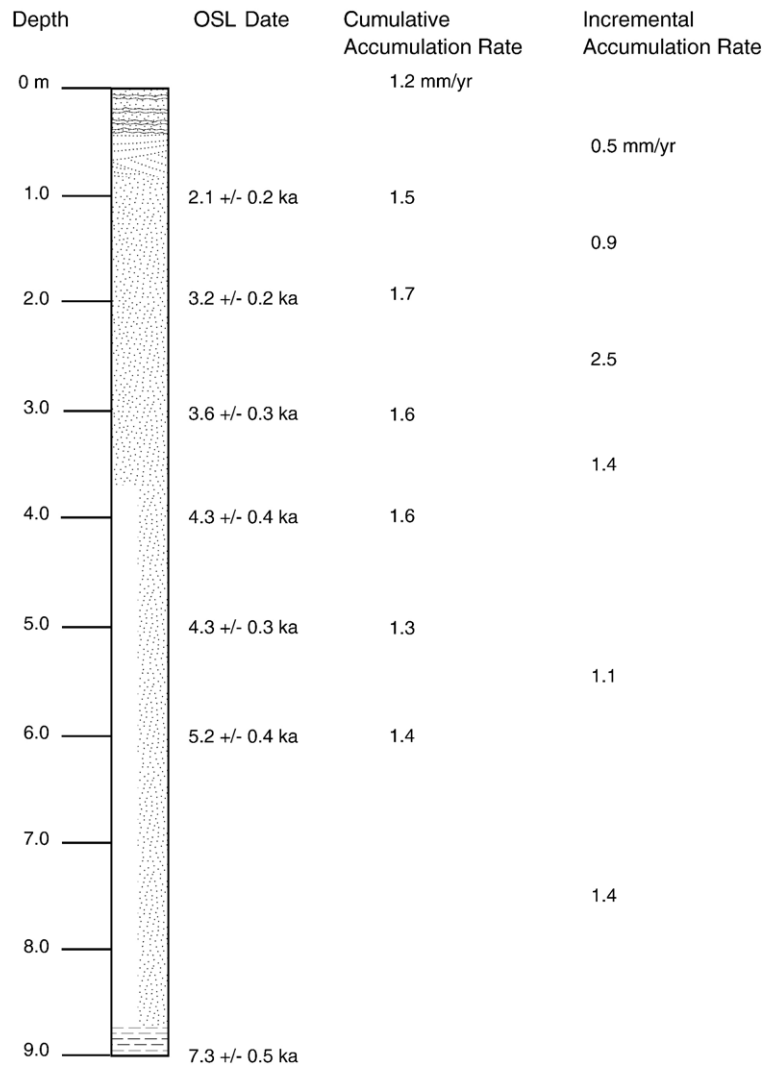
Fig. 14. OSL dates and calculated cumulative and incremental accumulation rates shown by depth in core UT-1. Cumulative rates calculated as thickness to a point divided by OSL age at that point progressively up the core. Incremental rates calculated by 1 m increments of thickness divided by the length of time to deposit this thickness.

results in a higher frequency of flooding in this area than elsewhere in the field; this may explain the higher degrees of interdune amalgamation reported by Simpson and Loope (1985) in their trenches located in a drier portion of the dune field.

The above analysis of accumulation rates, however, is clearly handicapped by a lack of detailed knowledge regarding the gypsum body (i.e., there is not yet a complete section), the nature of the dune field over time (i.e., has it been a wet aeolian system throughout its history?), and the cause of the water table rise that fosters accumulation. On the latter point, it is not known to what extent accumulation reflects an absolute rise of the water table because of climatic conditions versus a

relative rise in which the sediment column subsides through a static water table within this tectonically active basin. Alternatively, given its location within a topographic basin, it is possible that during arid deflationary periods the dune field existed as a dry aeolian system (see Kocurek and Havholm, 1994) in which accumulation occurred because of vertical flow expansion and a corresponding drop in the transport capacity of the wind (c.f., Simpson and Loope, 1985).

7. Conclusions

Based upon the OSL dates on samples from a core that penetrated the gypsum accumulation, Langford's

(2003) interpretation that the White Sands Dune Field originated at ∼7000 yr is reasonable. Working within his model, the dune field formed in response to the onset of progressively more arid conditions that caused a stepwise drop in the water table (i.e., lake level), which caused an increase in sediment availability of previously stored lacustrine sediment (i.e., lagged influx). A component of contemporaneous influx derived from gypsum precipitation from existing playas has probably occurred throughout the history of the dune field.

The current dune field is considered a wet aeolian system because the perched, shallow water table controls the behavior of the accumulation surface over time. The dune field also shows aspects of a stabilizing system because of surface cementation by gypsum, which acts primarily to slow deflation rates.

As determined from a monitored dune and its cross-strata, the wind regime yields a pattern of dune migration that is more complex than typically depicted. Dominant winds from the SW are transverse to the dune crests and account for most of the crest-normal migration, but a significant component of along-crest migration of the dune sinuosity to the SE occurs in response to oblique winds from the NW and N.

Trenches show dunes and interdune areas climbing at about 0.1°. Variation in scour depth corresponds to the streamwise length of the interdune areas, with a bias toward deflation of dune cross-strata and accumulation of interdune strata. This characteristic of White Sands is probably typical of wet aeolian systems where the water table fluctuates as part of the overall climate.

Within the trenches, dune sets show a consistent bundling of foresets between reactivation surfaces. Interpreted as annual cycles, subsets show progressive slipface progradation that is truncated by the bounding surfaces. In agreement with the monitored dune and its cross-strata, the cycles are interpreted to reflect the seasonal wind regime in which slipface development occurs during transverse winds from the SW and truncation occurs during periods of oblique winds from the NW and N. Also in agreement with the monitored dune and its cross-strata, the longest trench shows a transition from grainflow-dominated to wind-ripple-dominated cross-strata as would occur with the along-crest migration of the dune sinuosity.

Interdune accumulations similarly show annual cycles (varves) that correspond to the seasonal wet–dry periods. In one trench, a count of the interdune varves, as compared to the length of time the interdune has been an accumulation surface, shows that preservation is incomplete and probably most of the varve couplets have been removed by deflation or were never deposited. This extent of deflation is in agreement with the interpretation that scour of interdune areas occurs during dry periods.

Calculation of the recent accumulation rate based upon the angle of climb manifested in the trenches is significantly greater than the long-term accumulation rate determined from the nearby core. Aside from compaction and possible dissolution of gypsum, differences in the calculated accumulation rates may reflect significant variation in the accumulation rate over time and/or deflation of the accumulations over scales of time that vary from short term to unconformities in the geological sense.

Acknowledgements

References

Allen, J.R.L., 1970. A quantitative model of climbing ripples and their cross laminated deposits. Sedimentology 14, 5–26.

Allmendinger, R.J., 1972. Hydrologic control over the origin of gypsum at Lake Lucero, White Sands National Monument, New Mexico. M.S. Thesis, New Mexico Institute of Mining and Technology, Socorro, New Mexico. 182 pp.

Allmendinger, R.J., Titus, F.B., 1973. Regional hydrology and evaporative discharge as a present-day source of gypsum at White Sands National Monument, New Mexico. New Mexico Bureau Mines and Mineral Resources Open-File Report OF-55. 53 pp.

Beveridge, C., Kocurek, G., Ewing, R.C., Lancaster, N., Morthekau, P., Singhvi, A.S., Mahan, S.A., in press. Development of spatially diverse and complex dune-field patterns: Gran Desierto Dune Field, Sonora, Mexico. Sedimentology.

Crabaugh, M.M., 1994. Controls on accumulation in modern and ancient wet eolian systems. PhD Dissertation, University of Texas, Austin, Texas. 135 pp.

Ewing, R.C., Kocurek, G., Lake, L., 2006. Pattern analysis of dune-field parameters. Earth Surface Processes and Landforms 31, 1176–1191.

Frank, A., Kocurek, G., 1996. Toward a model for airflow on the lee side of aeolian dunes. Sedimentology 43, 451–458.

Fryberger, S.G., 2000. Geological overview of White Sands National Monument. http://www.nps.gov/whsa/Geology%20of%20White%20Sands/GeoHome.html.

Fryberger, S.G., Al-Sari, A.M., Clisham, T.J., Rizvi, S.A.R., Al-Hinai, K.G., 1984. Wind sedimentation in the Jafurah Sand Sea, Saudi Arabia. Sedimentology 31, 413–431.

Fryberger, S.G., Schenk, C.J., Krystinik, L.F., 1988. Stokes surfaces and the effects of near-surface groundwater-table on aeolian deposition. Sedimentology 35, 21–41.

Havholm, K.G., Kocurek, G., 1994. Factors controlling aeolian sequence stratigraphy: clues from super bounding surface features in the Middle Jurassic Page Sandstone. Sedimentology 41, 913–934.

Herrick, C.L., 1904. Lake Otero, an ancient salt lake basin in southeastern New Mexico. Economic Geology 4, 174–189.

Hunter, R.E., 1977a. Basic types of stratification in small eolian dunes. Sedimentology 24, 361–387.

Hunter, R.E., 1977b. Terminology of cross-stratified sedimentary layers and climbing-ripple structures. Journal of Sedimentary Petrology 47, 697–706.

Hunter, R.E., Rubin, D.M., 1983. Interpreting cyclic crossbedding, with an example from the Navajo Sandstone. In: Brookfield, M.E., Ahlbrandt, T.S. (Eds.), Eolian Sediments and Processes. Developments in Sedimentology, vol. 38. Elsevier, pp. 429–454.

Hunter, R.E., Richmond, B.M., Alpha, T.R., 1983. Storm-controlled oblique dunes of the Oregon coast. Bulletin Geological Society of America 94, 1450–1465.

Kocurek, G., 1981. Significance of interdune deposits and bounding surfaces in aeolian dune sands. Sedimentology 28, 753–780.

Kocurek, G., 1996. Desert aeolian systems, In: Reading, H.G. (Ed.), Sedimentary Environments: Processes, Facies and Stratigraphy, 3rd ed. Blackwell, Oxford, United Kingdom, pp. 125–153.

Kocurek, G., 1998. Aeolian system response to external forcing factors — a sequence stratigraphic view of the Saharan region. In: Alsharhan, A., Glennie, K., Whittle, G., Kendall, C. (Eds.), Quaternary Deserts and Climatic Change. A.A. Balkema, Rotterdam, The Netherlands, pp. 327–337.

Kocurek, G., Havholm, K.G., 1994. Eolian sequence stratigraphy — a conceptual framework. In: Weimer, P., Posamentier, H.W. (Eds.), Siliciclastic Sequence Stratigraphy. American Association Petroleum Geologists Memoir, vol. 58, pp. 393–409.

Kocurek, G., Lancaster, N., 1999. Aeolian system sediment state: theory and Mojave Desert Kelso dune field example. Sedimentology 46, 505–515.

Kocurek, G., Robinson, N.I., Sharp, J.M., 2001. The response of the water table in coastal aeolian systems to changes in sea level. Sedimentary Geology 139, 1–13.

Kottlowski, F.E., 1958. Lake Otero: second phase in formation of New Mexico's gypsum dunes. Geological Society of America Bulletin 69, 1733–1734.

Lancaster, N., Kocurek, G., Singhvi, A., Pandey, V., Deynoux, M., Ghienne, J.-F., 2002. Late Pleistocene and Holocene dune activity and wind regimes in the western Sahara of Mauritania. Geology 30, 991–994.

Langford, R.P., 2003. The Holocene history of the White Sands dune field and influences on eolian deflation and playa lakes. Quaternary International 104, 31–39.

McKee, E.D., 1966. Structures of dunes at White Sands National Monument, New Mexico (and a comparison with structures of dunes from other selected areas). Sedimentology 7, 1–69.

McKee, E.D., Douglass, J.R., 1971. Growth and movement of dunes at White Sands National Monument, New Mexico. U.S. Geological Survey Professional Paper 750-D, D108–D114.

McKee, E.D., Moiola, R.J., 1975. Geometry and growth of the White Sands Dune Field, New Mexico. U.S. Geological Survey Journal Research 3 (1), 59–66.

Murray, A.S., Wintle, A.G., 2000. Luminescence of dating of quartz using an improved single-aliquot regenerative-dose protocol. Radiation Measurements 32, 57–73.

Prescot, J.R., Hutton, J.T., 1994. Cosmic ray contribution to dose rates for luminescence and ESR dating: large depths and long-term variations. Radiation Measurements 23, 497–500.

Rubin, D.M., 1987. Cross-bedding, bedforms and Paleocurrents. Society of Economic Paleontologists and Mineralogists Concepts in Geology, vol. 1. 187 pp.

Rubin, D.M., Hunter, R.E., 1982. Bedform climbing in theory and nature. Sedimentology 29, 121–138.

Schenk, C.J., Fryberger, S.G., 1988. Early diagenesis of eolian dune and interdune sands at White Sands, New Mexico. Sedimentary Geology 55, 109–120.

Seager, W.R., Hawley, J.W., Kottlowski, F.E., Kelley, S.A., 1987. Geology of east half of Las Cruces and northeast El Paso 1° × 2° sheets, New Mexico. New Mexico Bureau of Mines and Mineral Resources Geologic Map, vol. 57.

Simpson, E.L., Loope, D.B., 1985. Amalgamated interdune deposits, White Sands, New Mexico. Journal of Sedimentary Petrology 55 (3), 361–365.